Chapter 5

Output Feedback Based Discrete-Time Sliding Mode Control Using Minima Operator

5.1 Introduction

Often in practical applications, variations in dynamics across different channels, along with hardware constraints on specific input-output pairs, often necessitate the use of multiple rates. Multirate systems provide the advantage of maintaining performance while operating at lower sampling frequencies compared to single-rate systems. This characteristic is particularly crucial in networked control systems, where bandwidth limitations impose constraints on sampling rates. Extensive research has explored the challenges associated with static output feedback and fast output sampling (FOS) [31], [36,37]. MROF presents an alternative approach that relies solely on measured output readings and prior input signals, offering a practical and effective solution.

In [36], FOS feedback is introduced, which encompasses the characteristics of static output feedback while offering the flexibility to arbitrarily allocate system poles and ensure the stabilization of controlled dynamics. In the FOS method, every measurement duration $\mathtt{t}$ is partitioned into $\mathbb{M}$ subintervals $\mathtt{t}_o = \mathtt{t}/\mathbb{M}$. The value of $\mathbb{M}$ should be selected such that $\mathbb{M} \geq O$, where O is the observability index. The latest $\mathbb{M}$ output measurements are recorded at time interval $t = l\mathtt{t}_o$, where, $l = 0, 1, \ldots,$ and a constant control signal is maintained throughout $\mathtt{t}$. This input signal is formed as a linear aggregate of the last $\mathbb{M}$

output measurements. In [30], authors utilizing a periodic intermittent control combined with the MROF technique aim to robustly stabilize discretized linear time-invariant systems, thereby redefining the concept of discrete-time sliding mode. In [31], a proposed method for attaining quasi-sliding mode (QSM) based on Gao's law in uncertain systems employs a rapid output sampling control strategy that eliminates control switching and consequently minimizes chattering.

The objective is to implement DSMC for the system by driving its states toward the designated sliding surface. Upon reaching the vicinity of this surface, the focus shifts to ensuring that the system states remain confined within the neighborhood of the sliding surface. A solution to this problem using state feedback has been proposed in [2]. However, since the states are seldom available for feedback, output feedback control is typically required. Consequently, the problem now involves achieving QSMC using only the system's output. As noted in [55], a static output feedback solution is not always feasible. In this paper, we propose two discrete-time output-feedback SMC algorithms for systems with bounded uncertainty, incorporating the following contributions:

- The proposed algorithms are based on Minima operator-Based Reaching Laws and FOS based feedback.
- The design integrates features of multi-rate output systems and ensures finite-time reachability to sliding surface.
- The algorithm operates on the measured system output, with the control input computed solely from previous output measurements and the most recent control signal.
- The settling time can be explicitly estimated based on initial conditions.

Consider a DTS of order n, with sampling time $\mathtt{t}$ seconds:

$$z(k+1) = A_{\mathtt{t}} z(k) + \Gamma_{\mathtt{t}} u(k) + \tilde{\delta}(k) \quad y(k) = Cz(k) \tag{5.1}$$

Here, the state $z(k) \in \mathbb{R}^n$, $\tilde{\delta}(k)$ represents a vector that captures unaccounted dynamics and extrinsic disturbances within the system, $y(k)$ represents the output of the system and $k \in \mathbb{Z}$ is an integer. It is considered that $\tilde{\delta}(k) = 0$ for all $k < 0$. The matrices $A_{\mathtt{t}}$, $\Gamma_{\mathtt{t}}$,

and C are properly sized, ensuring compatibility, where $(A_{\mathtt{t}}, \Gamma_{\mathtt{t}})$ exhibits controllability, and $(A_{\mathtt{t}}, C)$ showcases observability.

We propose the sliding function as $\aleph(k) := \alpha(z(k))$, and corresponding sliding surface by the contour set $\alpha^{-1}(0) := \{z \in D : \alpha(z) = 0\}$. For our discussion purpose, switching function is characterized as:

$$\aleph(k) = b^T z(k), \tag{5.2}$$

where $b \in \mathbb{R}^{n\times 1}$ with $b^T\Gamma_{\mathtt{t}} \neq 0$. Consider bounded matched-type perturbation such that $b^T\tilde{\delta}(k) = \delta(k)$ and $\delta_l \leq \delta(k) \leq \delta_u$, where $\delta_l, \delta_u \in \mathbb{R}$ are known a priori bounds. Additionally, the following relationships hold: $\delta_0 = \frac{\delta_l+\delta_u}{2}$ represents the mean value of $\delta(k)$, and $\delta_d = \frac{\delta_u-\delta_l}{2}$ denotes the variation from the mean value of $\delta(k)$.

5.2 State and Output Relation for Multirate Uncertain System

Examine the system outlined in equation (5.1) captured with a sampling period $\mathtt{t}_o = \mathtt{t}/\mathbb{M}$, where $\mathbb{M} \in Z \geq O$. Consider this system described by the matrices A, Γ, and C. Suppose the system's output is recorded in every $\mathtt{t}_o$ seconds, while the input is applied in every $\mathtt{t}$ seconds. Consider that the disturbance vector in the system described by equation (5.1) influences the dynamics of the $\mathtt{t}_o$ system as follows:

$$\begin{aligned} z(k\mathtt{t} + (i+1)\mathtt{t}_o) &= Az(k\mathtt{t} + i\mathtt{t}_o) + \Gamma u(k\mathtt{t}) + \delta'(k) \\ y(k\mathtt{t} + i\mathtt{t}_o) &= Cz(k\mathtt{t} + i\mathtt{t}_o), \end{aligned} \tag{5.3}$$

where $\delta'(k)$ represents the perturbation in the $\mathtt{t}_o$ system resulting from $\tilde{\delta}(k)$. By applying equations (5.3), the state vector at $i = 0, 1, \ldots, \mathbb{M}-1$ can be expressed in terms of $z(k\mathtt{t})$ as shown below:

$$\begin{aligned} z(k\mathtt{t} + \mathtt{t}_0) &= Az(k\mathtt{t}) + \Gamma u(k\mathtt{t}) + \delta'(k). \\ z(k\mathtt{t} + 2\mathtt{t}_0) &= Az(k\mathtt{t} + \mathtt{t}_0) + \Gamma u(k\mathtt{t}) + \delta'(k). \\ &= A^2 z(k\mathtt{t}) + (A\Gamma + \Gamma)u(k\mathtt{t}) \\ &\quad + A\delta'(k) + \delta'(k). \\ &\vdots \\ z((k+1)\mathtt{t} - \mathtt{t}_0) &= A^{\mathbb{M}-1} z(k\mathtt{t}) + \sum_{i=0}^{\mathbb{M}-2} A^i \Gamma u(k\mathtt{t}) + \sum_{i=0}^{\mathbb{M}-2} A^i \delta'(k). \end{aligned}$$

$$z((k+1)\mathtt{t}) = A^{\mathbb{M}} z(k\mathtt{t}) + \sum_{i=0}^{\mathbb{M}-1} A^i \Gamma u(k\mathtt{t}) + \sum_{i=0}^{\mathbb{M}-1} A^i \delta'(k). \tag{5.4}$$

By harnessing the features of Linear time invariant systems in discrete time and juxtaposing equation (5.4) to equation (5.1), we derive the following:

$$\delta'(k) = \left(\sum_{i=0}^{\mathbb{M}-1} A^i \right)^{-1} \tilde{\delta}(k) \tag{5.5}$$

This leads to the relationship between the system states $z(k)$ and the lifted output y_{k+1} as follows:

$$\begin{aligned} z((k+1)\mathtt{t}) &= A_{\mathtt{t}} z(k\mathtt{t}) + \Gamma_{\mathtt{t}} u(k\mathtt{t}) + \tilde{\delta}(k) \\ y_{k+1} &= C_0 z(k) + D_0 u(k) + C_\delta \tilde{\delta}(k). \end{aligned} \tag{5.6}$$

where,

$$y_k = \begin{bmatrix} y((k-1)\mathtt{t}) \\ y((k-1)\mathtt{t} + \mathtt{t}_o) \\ \vdots \\ y(k\mathtt{t} - \mathtt{t}_o) \end{bmatrix}, C_0 = \begin{bmatrix} C \\ CA \\ CA^2 \\ \vdots \\ CA^{\mathbb{M}-1} \end{bmatrix},$$

$$D_0 = \begin{bmatrix} 0 \\ C\Gamma \\ C(A\Gamma + \Gamma) \\ \vdots \\ \sum_{i=0}^{\mathbb{M}-2} CA^i\Gamma \end{bmatrix}, C_\delta = \begin{bmatrix} 0 \\ C \\ CA + C \\ \vdots \\ \sum_{i=0}^{\mathbb{M}-2} CA^i \end{bmatrix}.$$

Remark 5.1 *Equation* (5.6) *represents the relationship between the lifted output and system states using* (5.1), (5.4), *and* (5.5) *[36].*

Thus, we have the relation:

$$\mathbf{C}_0^T \mathbf{y}_{t+1} = \mathbf{C}_0^T (\mathbf{C}_0 z(k) + \mathbf{D}_0 u(k) + \mathbf{C}_\delta \tilde{\delta}(k)). \tag{5.7}$$

Hence, using (5.6), the state $z(k+1)$ can be inferred as:

$$z(k+1) = B_y \mathbf{y}_{k+1} + B_u u(k) + B_\delta \tilde{\delta}(k) \tag{5.8}$$

where:

$$\begin{aligned} B_y &= A_{\mathtt{t}} \left(\mathbf{C}_0^T \mathbf{C}_0\right)^{-1} \mathbf{C}_0^T, \\ B_u &= \Gamma_{\mathtt{t}} - A_{\mathtt{t}} \left(\mathbf{C}_0^T \mathbf{C}_0\right)^{-1} \mathbf{C}_0^T \mathbf{D}_0, \\ B_\delta &= I - A_{\mathtt{t}} \left(\mathbf{C}_0^T \mathbf{C}_0\right)^{-1} \mathbf{C}_0^T \mathbf{C}_\delta. \end{aligned} \tag{5.9}$$

Thus, the state $z(k)$ can be expressed using the lifted output vector $\mathbf{y}_k$ as:

$$z(k) = B_y \mathbf{y}_k + B_u u(k-1) + B_\delta \tilde{\delta}(k-1). \tag{5.10}$$

5.3 Multirate Output Control Scheme Based on Modified RL

Consider the system represented by equations (5.6). Let's introduce a new variable, $\eta(k)$, defined as follows

$$\eta(k) = b^T A_{\mathtt{t}} B_\delta \tilde{\delta}(k) \tag{5.11}$$

Since the perturbation is bounded, we also have $\eta_l \leq \eta(k) \leq \eta_u$ and $\eta_m = \max\left(|\eta_l|, |\eta_u|\right)$. Also define the QSM band as $\omega_m = \delta_m + \eta_m$, here, δ_m as defined as $\delta_l < \delta(k) < \delta_u$ and $\max\{|\delta_l|, |\delta_u|\} = \delta_m$.

Motivated by RL1, we defined modified RL (MRL1) as

$$\aleph(k+1) = \aleph(k) - \varsigma \text{sign}[\aleph(k)] \min\left(\frac{|\aleph(k)|}{\varsigma}, |\aleph(k)|^\beta\right) + \delta(k) + \eta(k-1). \tag{5.12}$$

Theorem 5.2 *Consider the system described by* (5.6) *and using MRL* (5.12) *and*

$$u(k) = -(b^T \Gamma_{\mathtt{t}})^{-1} \left[b^T A_{\mathtt{t}} (B_y \mathbf{y}_k + B_u u(k-1) - \aleph(k) + \varsigma sign[\aleph(k)] \min\left(\frac{|\aleph(k)|}{\varsigma}, |\aleph(k)|^\beta\right) \right] \tag{5.13}$$

using control input (5.13) *the system's switching function magnitude is ultimately bounded by* ω_m. *Also, it enters in ultimate band for some* $k \leq I(\aleph(0))$
where $I(\aleph(0)) \leq \left\lceil \log_{\left[1-\varsigma|\aleph(0)|^{\beta-1}+\omega_m|\aleph(0)|^{-1}\right]} \frac{\varsigma^{\frac{1}{1-\beta}}}{|\aleph(0)|} \right\rceil + 1$

Proof

Consider the switching function (5.2),

$$\aleph(k+1) = b^T z(k+1),$$

Consider the system described by (5.6) and MRL (5.12).

$$b^T(A_{\mathtt{t}}z(k)+\Gamma_{\mathtt{t}}u(k)+\tilde{\delta}(k))=\aleph(k)-\varsigma\text{sign}[\aleph(k)]\min\left(\frac{|\aleph(k)|}{\varsigma},|\aleph(k)|^{\beta}\right)+\delta(k)+\eta(k-1)$$

$$b^TA_{\mathtt{t}}z(k)+b^T\Gamma_{\mathtt{t}}u(k)+b^T\tilde{\delta}(k)=\aleph(k)-\varsigma\,\text{sign}[\aleph(k)]\min\left(\frac{|\aleph(k)|}{\varsigma},|\aleph(k)|^{\beta}\right)+\delta(k)+\eta(k-1) \tag{5.14}$$

Using equation (5.8)

$$b^TA_{\mathtt{t}}(B_y\mathbf{y}_k+B_uu(k-1)+B_d\tilde{\delta}(k-1))+b^T\Gamma_{\mathtt{t}}u(k)=\aleph(k)-\varsigma\text{sign}[\aleph(k)]\min\left(\frac{|\aleph(k)|}{\varsigma},|\aleph(k)|^{\beta}\right)$$

$$+\eta(k-1)$$

$$b^TA_{\mathtt{t}}(B_y\mathbf{y}_k+B_uu(k-1))+b^T\Gamma_{\mathtt{t}}u(k)=\aleph(k)-\varsigma\text{sign}[\aleph(k)]\min\left(\frac{|\aleph(k)|}{\varsigma},|\aleph(k)|^{\beta}\right)$$

At this point, the control input can be determined as follows:

$$u(k)=-(b^T\Gamma_{\mathtt{t}})^{-1}\left[b^TA_{\mathtt{t}}(B_y\mathbf{y}_k+B_uu(k-1)-\aleph(k)+\varsigma\text{sign}[\aleph(k)]\min\left(\frac{|\aleph(k)|}{\varsigma},|\aleph(k)|^{\beta}\right)\right] \tag{5.15}$$

Thus, the control input can be determined utilizing previous output samples along with the most recent input signal. However, at $k=0$, no preceding outputs are available for control purposes. Therefore, referring to equation (5.15), and assuming the system is unaffected by disturbances before $k=0$, and with initial state $z(0)$ and the corresponding $\aleph(0)$ are considered.

$$u(0)=-(b^T\Gamma_{\mathtt{t}})^{-1}\left[b^TA_{\mathtt{t}}(z(0))-\aleph(0)+\varsigma\text{sign}[\aleph(0)]\min\left(\frac{|\aleph(0)|}{\varsigma},|\aleph(0)|^{\beta}\right)\right] \tag{5.16}$$

When the control input obtained from equation (5.15) is implemented within the system (5.6), the system adheres to the MRL1:

$$\aleph(k+1)=\aleph(k)-\varsigma\text{sign}[\aleph(k)]\min\left(\frac{|\aleph(k)|}{\varsigma},|\aleph(k)|^{\beta}\right)+\delta(k)+\eta(k-1).$$

Considering the trivial scenario, if $\frac{|\aleph(k)|}{\varsigma}\leq|\aleph(k)|^{\beta}$, then we will have in next step

$$\aleph(k+1)=\aleph(k)-\varsigma\text{sign}[\aleph(k)]|\aleph(k)|+\delta(k)+\eta(k-1)$$

$$\Rightarrow\aleph(k+1)=\delta(k)+\eta(k-1)$$

Therefore, we derive
$|\aleph(k+1)| \leq \omega_m$, , with $I(\aleph(0)) = 1$. Moreover, for all $k \geq I(\aleph(0))$, $|\aleph(k)| \leq \omega_m$, demonstrating the presence of QSM. The next scenario, if $\frac{|\aleph(k)|}{\varsigma} > |\aleph(k)|^{\beta}$, then

$$\aleph(k+1) = \aleph(k) - \varsigma \text{sign}[\aleph(k)]|\aleph(k)|^{\beta} + \delta(k) + \eta(k-1).$$

We can further write,

$$|\aleph(k+1)| = |\aleph(k) - \varsigma \text{sign}[\aleph(k)]|\aleph(k)|^{\beta} + \delta(k) + \eta(k-1)|.$$

Since $|\aleph(k)| > |\aleph(k)|^{\beta}$, it follows that,

$$|\aleph(k+1)| \leq |\aleph(k)| - \varsigma|\aleph(k)|^{\beta} + \omega_m.$$

Additionally, it can be expressed as

$$\begin{aligned}
|\aleph(k)| &\leq |\aleph(k-1)|(1 - \varsigma|\aleph(k-1)|^{\beta-1} + \omega_m|\aleph(k-1)|^{-1}) \\
&\vdots \\
&\leq |\aleph(0)|(1 - \varsigma|\aleph(0)|^{\beta-1} + \omega_m|\aleph(0)|^{-1}) \dots \\
&(1 - \varsigma|\aleph(k-1)|^{\beta-1} + \omega_m|\aleph(k-1)|^{-1}) \\
&\vdots
\end{aligned}$$

$$|\aleph(k)| \leq |\aleph(0)|(1 - \varsigma|\aleph(0)|^{\beta-1} + \omega_m|\aleph(0)|^{-1})^k \tag{5.17}$$

If $||\aleph(0)|(1-\varsigma|\aleph(0)|^{\beta-1} + \omega_m|\aleph(0)|^{-1})^k| \leq \varsigma|\aleph(k)|^{\beta}$, then from (5.18), $|\aleph(k)| \leq \varsigma|\aleph(k)|^{\beta} \Rightarrow |\aleph(k+1)| \leq \omega_m, \forall k \geq \left\lceil \log_{\left[1-\varsigma|\aleph(0)|^{\beta-1}+\omega_m|\aleph(0)|^{-1}\right]} \frac{\varsigma^{\frac{1}{1-\beta}}}{|\aleph(0)|} \right\rceil + 1$. Moreover, the settling time expression is given by

$$I(\aleph(0)) \leq \left\lceil \log_{\left[1-\varsigma|\aleph(0)|^{\beta-1}+\omega_m|\aleph(0)|^{-1}\right]} \frac{\varsigma^{\frac{1}{1-\beta}}}{|\aleph(0)|} \right\rceil + 1$$

Therefore, it is concluded that the modulus of the switching function has an ultimate bound ω_m, which is achieved in a finite number of time steps.

Remark 5.3 *The computation of the control input* (5.15) *relies on past output samples and the most recent input signal. Additionally, the use of the lifted output signal effectively eliminates the dependence on state information, as outlined in* (5.10).

Corollary 5.4 *The DTS* (5.1) *satisfies the QSM reaching condition in the neighborhood of the set* $\alpha^{-1}(0)$ *if, for some* $k \geq 0$*, the following conditions hold:*

$$\frac{|\aleph(k)|}{\varsigma} > |\aleph(k)|^{\beta} \Rightarrow |\aleph(k+1)| < |\aleph(k)| - \varepsilon$$
$$\frac{|\aleph(k)|}{\varsigma} \leq |\aleph(k)|^{\beta} \Rightarrow 0 \leq |\aleph(k+1)| \leq \omega_m$$

where $\varepsilon \in \mathbb{R}^+$ *is arbitrarily small.*

In the following section, we will focus on the development of the controller and conduct a detailed analysis for the special case of the reaching law RL1, which was previously defined as RL2. We have proposed a new modified reaching law, MRL2, based on RL2 by integrating its features with the MROF. Furthermore, we have outlined the conditions under which the results of MRL2 converge with those of MRL1. Consider the MRL2 defined as

$$\aleph(k+1) = \aleph(k) - \text{sign}[\aleph(k)] \min(|\aleph(k)|, \varsigma) + \delta(k) + \eta(k-1) \tag{5.18}$$

Here $\varsigma \in R+$ is selected s.t. $\varsigma \geq \omega_m$.

Theorem 5.5 *Consider the system described by* (5.6) *and using MRL* (5.18)*, and*

$$u(k) = -(b^T \Gamma_{\mathtt{t}})^{-1} \left[b^T A_{\mathtt{t}} (B_y \mathbf{y}_k + B_u u(k-1)) - \aleph(k) + sign[\aleph(k)] \min\left(|\aleph(k)|, \varsigma\right) \right] \tag{5.19}$$

When applying the control input given in equation (5.19)*, the switching function of the system is ultimately bounded by* $\omega_m = \delta_m + \eta_m$*. Also, it enters in ultimate band for some* $k \leq I(\aleph(0))$ *where*

$$I(\aleph(0)) \leq \left\lceil \frac{|\aleph(0)| - \omega_m}{\varsigma - \omega_m} \right\rceil.$$

Proof

Using switching function (5.2),

$$\aleph(k+1) = b^T z(k+1),$$

Consider the system described by (5.6) and MRL2 (5.18).

$$b^T(A_{\mathtt{t}}z(k) + \Gamma_{\mathtt{t}}u(k) + \tilde{\delta}(k)) = \aleph(k) - \text{sign}[\aleph(k)]\min(|\aleph(k)|, \varsigma) + \delta(k) + \eta(k-1)$$
$$b^T A_{\mathtt{t}}z(k) + b^T\Gamma_{\mathtt{t}}u(k) = \aleph(k) - \text{sign}[\aleph(k)]\min(|\aleph(k)|, \varsigma) + \eta(k-1)$$

Using equation (5.8)

$$b^T A_{\mathtt{t}}(B_y\mathbf{y}_k + B_u u(k-1) + L_d\tilde{\delta}(k-1)) + b^T\Gamma_{\mathtt{t}}u(k) = \aleph(k) - \text{sign}[\aleph(k)]\min(|\aleph(k)|, \varsigma) + \eta(k-1)$$
$$b^T A_{\mathtt{t}}(B_y\mathbf{y}_k + B_u u(k-1)) + b^T\Gamma_{\mathtt{t}}u(k) = \aleph(k) - \text{sign}[\aleph(k)]\min(|\aleph(k)|, \varsigma)$$

At this point, the control input can be determined as follows:

$$u(k) = -(b^T\Gamma_{\mathtt{t}})^{-1}\left[b^T A_{\mathtt{t}}(B_y\mathbf{y}_k + B_u u(k-1)) - \aleph(k) + \text{sign}[\aleph(k)]\min\left(|\aleph(k)|, \varsigma\right)\right] \tag{5.20}$$

Thus, the control input can be determined utilizing previous output samples along with the most recent input signal. However, at $k = 0$, no preceding outputs are available for control purposes. Consequently, using equation (5.18) and based on the assumption that no disturbances before $k = 0$ influence the system, and by assuming an initial state $z(0)$ and corresponding $\aleph(0)$ we have,

$$u(0) = -(b^T\Gamma_{\mathtt{t}})^{-1}\left[b^T A_{\mathtt{t}}(z(0)) - \aleph(k) + \text{sign}[\aleph(0)]\min(|\aleph(0)|, \varsigma)\right]$$

Now, when the control input obtained from equation (5.20) is implemented within the system (5.6), the system adheres to the MRL2.

$$\aleph(k+1) = \aleph(k) - \text{sign}[\aleph(k)]\min(|\aleph(k)|, \varsigma) + \delta(k) + \eta(k-1)$$

Consider the scenario where $|\aleph(k)| \leq \varsigma$, then $\aleph(k+1) = \delta(k) + \eta(k-1)$ implies in the next step $|\aleph(k+1)| \leq \delta(k) + \eta(k-2)|$. Consequently, $|\aleph(k+1)| \leq \omega_m$, with $I(\aleph(0)) = 1$. Moreover, for all $k \geq I(\aleph(0))$, $|\aleph(k)| \leq \omega_m$, demonstrating the existence of QSM.

For another scenario, if $|\aleph(k)| > \varsigma$, then $|\aleph(k+1)| \leq |\aleph(k) - \text{sign}[\aleph(k)]\varsigma + \delta(k) + \eta(k-1)|$. As $|\aleph(k)| > \varsigma$, it follows that $|\aleph(k+1)| \leq |\aleph(k)| - \varsigma + \omega_m$. Additionally, it can

be deduced as:

$$\begin{aligned}
|\aleph(k)| &\leq |\aleph(k-1)| - \varsigma + \omega_m \\
&\leq |\aleph(k-2)| - 2(\varsigma - \omega_m) \\
&\leq \\
&\vdots \\
&\leq |\aleph(0)| - k(\varsigma - \omega_m)
\end{aligned}$$

If $(|\aleph(0)| - k(\varsigma - \omega_m)) \leq \varsigma$, then $|\aleph(k)| \leq \varsigma$, implying $|\aleph(k+1)| \leq \omega_m$ for all $k \geq \frac{|\aleph(0)|-\omega_m}{\varsigma-\omega_m}$. The settling time function is $I(\aleph(0)) = \left\lceil \frac{|\aleph(0)|-\omega_m}{\varsigma-\omega_m} \right\rceil$. Therefore, it is concluded that $|\aleph(k)| \leq \omega_m$ within finite time steps.

Corollary 5.6 *The QSM in the vicinity of the set $\alpha^{-1}(0)$ when $|\aleph(k)| \leq \omega_m = \delta_m + \eta_m$.*

Corollary 5.7 *The system described by equation (5.1) satisfies the QSM reaching condition in the vicinity of $\alpha^{-1}(0)$ if, for some $k \geq 0$, the following conditions are met:*

$$\begin{aligned}
&|\aleph(k)| > \varsigma \Rightarrow |\aleph(k+1)| < |\aleph(k)| - \varepsilon; \\
&|\aleph(k)| \leq \varsigma \Rightarrow 0 \leq |\aleph(k+1)| \leq \omega_m,
\end{aligned} \tag{5.21}$$

where $\varepsilon \in \mathbb{R}^+$ is arbitrarily small.

Remark 5.8 *In control law (5.15), setting ς to 1 and keeping β very close to zero results in behavior similar to control law (5.20) with $\varsigma = 1$. The interaction between ς and β influences the convergence of the switching function. Smaller values of ς and β lead to slower convergence, while keeping β close to 1 and ς large ensures rapid convergence of the switching function. Furthermore, the selection of ς and β for various applications can be tailored based on the actuator saturation limits of the respective systems.*

Remark 5.9 *Corollary 1 aligns with the ideal sliding mode definition for continuous-time systems when $\delta(k) = 0$, as $\aleph(k)$ converges exactly to $\alpha^{-1}(0)$ and remains there indefinitely.*

Remark 5.10 *The control input (5.20) can be computed using past output samples in conjunction with the most recent input signal. Moreover, by utilizing the lifted output signal, we effectively mitigate the need for state information as described in (5.10).*

5.4 Result and Discussion

The effectiveness of the proposed control strategy is evaluated by analyzing its performance in a given example. The obtained results are then bench-marked against two existing approaches: the state feedback-based method outlined in [2] and the MROF methodology detailed in [3]. This comparative assessment provides insights into the relative advantages and potential improvements offered by the proposed strategy.

Example 5.11 *[56] Consider the DTS of smart-structure beams:*

$$z(k+1) = \begin{pmatrix} 0 & 1 \\ 0.4 & -0.3 \end{pmatrix} z(k) + \begin{pmatrix} 0 \\ 1 \end{pmatrix} u(k) + \begin{pmatrix} 0 \\ \sin\left(\frac{k}{2}\right)\exp\left(-\frac{k}{5}\right) \end{pmatrix};$$
$$y(k) = [1\ 0]z(k).$$

5.4.1 Comparative Study with State Feedback

In [2], the authors presented two RL-based DSMC methods, as mentioned in Section II. For the sake of comparison, we have used the state feedback control law derived from these algorithms to compare with the proposed fast output sampling sliding mode control laws.

State Feedback Control Based on RL1

A control signal was created using RL1, and the resulting state feedback control follows this structure:

$$u_1(k) = \left(b^T\Gamma_{\mathtt{t}}\right)^{-1}\left[-b^T A_{\mathtt{t}} z(k) + \aleph(k) - sign[\aleph(k)]\min\left(|\aleph(k)|, \varsigma\right)\right] \tag{5.22}$$

The system input is sampled at $T = 0.2$ sec, and the resulting state feedback-based control utilizes a sliding function defined as $\aleph(k) = b^T z(k)$, where $b^T = [-0.4\ 1]$. Additionally, the control gain $\varsigma = 0.8$ is used.

State Feedback Control Based on RL2

Additionally, another control signal was crafted using RL2, and the resulting state feedback control law follows this structure:

$$u_2(k) = \left(b^T\Gamma_{\mathtt{t}}\right)^{-1}\left[-b^T A_{\mathtt{t}} z(k) + \aleph(k) - \varsigma sign[\aleph(k)]\min\left(\frac{|\aleph(k)|}{\varsigma}, |\aleph(k)|^{\beta}\right)\right] \tag{5.23}$$

The sampling interval and sliding function are the same as those used in the state feedback control $u_1(k)$, while other parameters are set to $\varsigma = 0.8$ and $\beta = 0.1$.

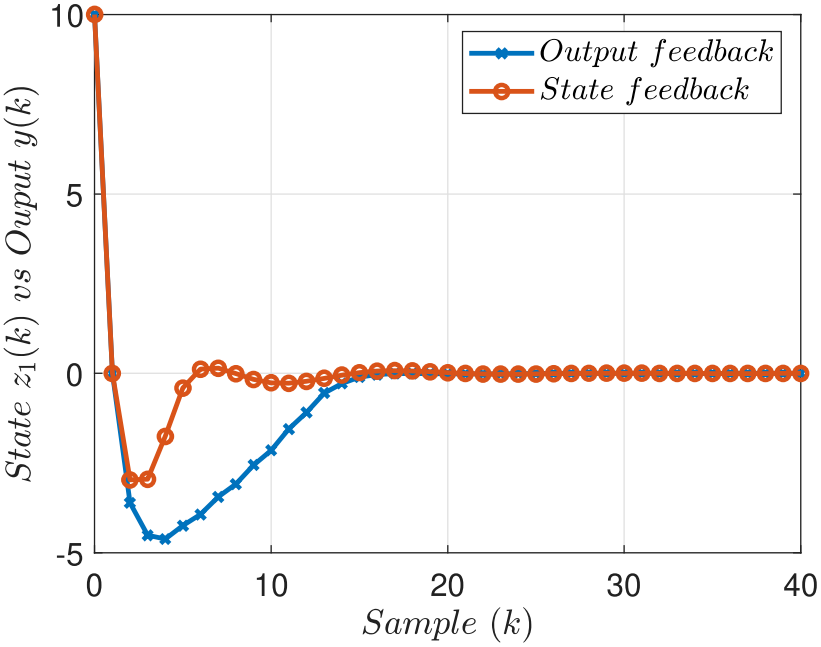

(a) MRL1 simulation result vs RL 1 [2]

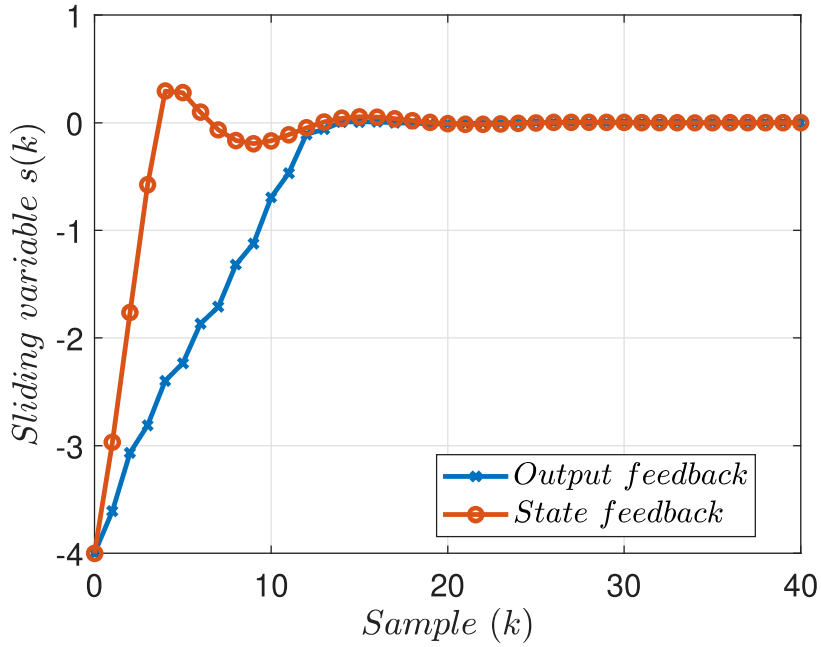

(b) MRL1 vs RL1 sliding variable [2]

Figure 5.1: MRL1 simulation result vs RL1 [2]

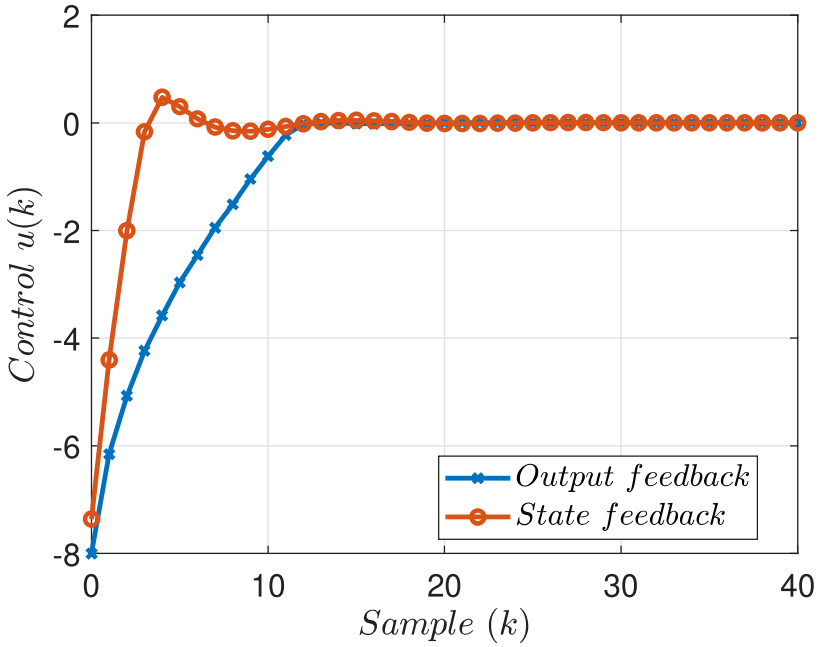

(a) Control input $u(k)$: MRL1 vs RL1 [2]

Figure 5.2: Comparison of control performance for MRL1 vs RL1 [2].

Proposed Multirate Output Feedback Based Control Law MRL1 and MRL2

The developed control laws use sliding line, same as above for the sake of comparison. Computation of the parameters:

$$B_y = \begin{pmatrix} 5.407 & -6.94 \\ -1.222 & 2.082 \end{pmatrix}, \quad B_u = \begin{pmatrix} 2.814 \\ 0.156 \end{pmatrix}, \quad B_d = \begin{pmatrix} 7.94 & 0 \\ -2.082 & 1 \end{pmatrix}$$

The system output is sampled at a frequency twice that of the input sampling rate. The sliding surfaces are designed such that one of them coincides with the sliding surface used in the state feedback approach, ensuring a meaningful basis for comparison. For consistency, the parameters ς and β are set identical to those in the state feedback control law.

Fig. 5.1a, Fig. 5.1b and Fig. 5.2a presents the simulation results for a time-varying disturbance applied to MRL1, depicting the evolution of the sliding function $\aleph(k)$, output $y(k)$, and control input $u(k)$. This figure facilitates a comparative analysis between the proposed MRL1-based controller and the state feedback sliding mode control method outlined in [2]. The results show that the state trajectory progressively converges toward

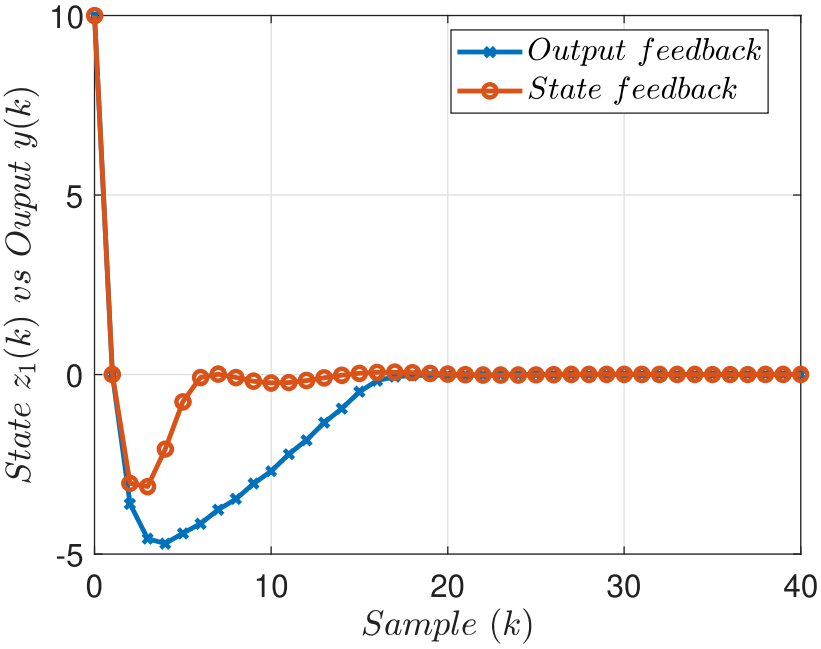

(a) MRL2 simulation result vs RL 2 [2]

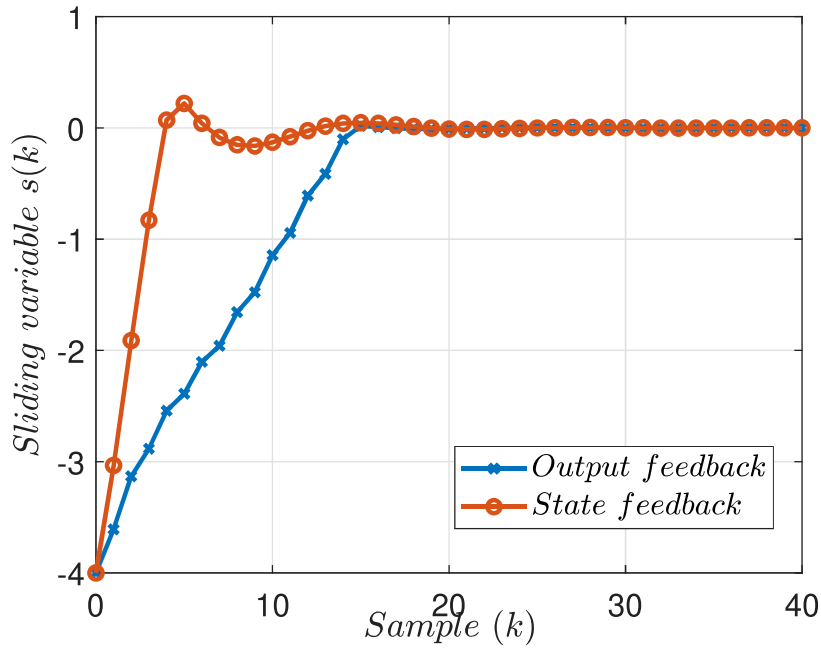

(b) MRL2 vs RL2 sliding variable [2]

Figure 5.3: MRL1 simulation result vs RL1 [2]

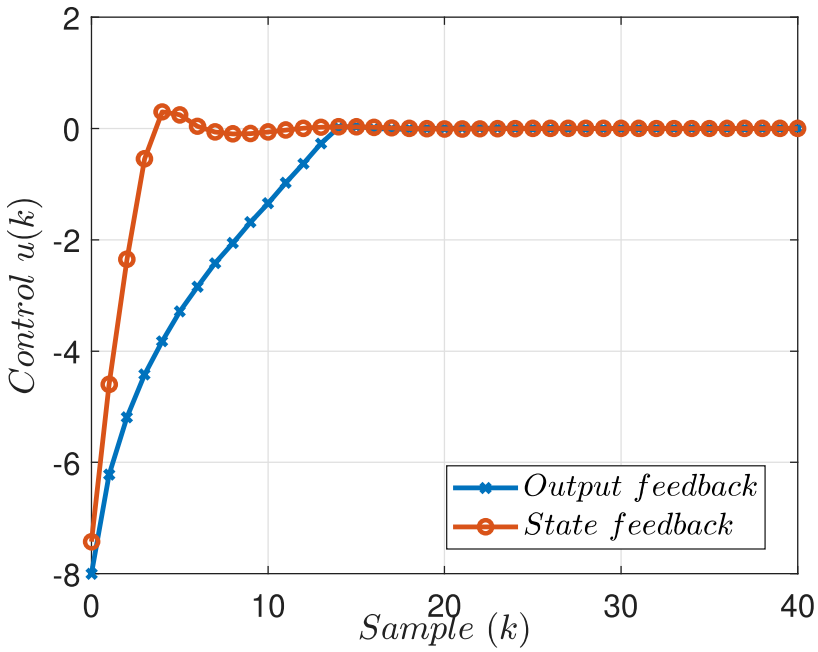

(a) Control input $u(k)$: MRL2 vs RL2 [2]

Figure 5.4: Comparison of control performance for MRL2 vs RL2 [2].

the quasi-sliding mode band.

Similarly, Fig. 5.3a, Fig. 5.3b and Fig. 5.4a illustrates the behavior of the sliding function $\aleph(k)$, output $y(k)$, and control input $u(k)$ for MRL2, offering a comparative assessment with the state feedback sliding mode control approach described in [2]. The findings indicate that while the proposed controller exhibits a longer settling time than the state feedback sliding mode control—primarily due to the absence of full state information—it significantly reduces the quasi-sliding mode band.

5.4.2 Comparative Study with MROF

In [3], the authors introduced MROF-based DSMC methods. To further validate these results, we compare the output feedback control law derived from these algorithms with the two proposed fast output sampling sliding mode control laws. The MROF output control law used in [3] is given by

$$u(k) = \begin{bmatrix} -3.019 & 4.233 \end{bmatrix} y(k) - 1.017u(k-1) + s_d(k+1) - 0.06.$$

Here, $s_d(k)$ is a priori known; for further details, readers may refer to [3]. Fig. 5.5a, Fig. 5.6a and Fig. 5.7a & table 1 presents a comparison between MRL1 and MRL2 with the results in [3] for $k_1 = 10$, demonstrating that both proposed algorithms exhibit nearly identical settling times. This comparison clearly highlights the reduced quasi-sliding mode band.

Table 5.1

Control Methods	**Control input steady state**	**Settling time**	**Sliding variable**
MRL1	0.001	11	0.0009
MRL2	0.001	6	0.0009
[28]	-0.1	10	-0.08

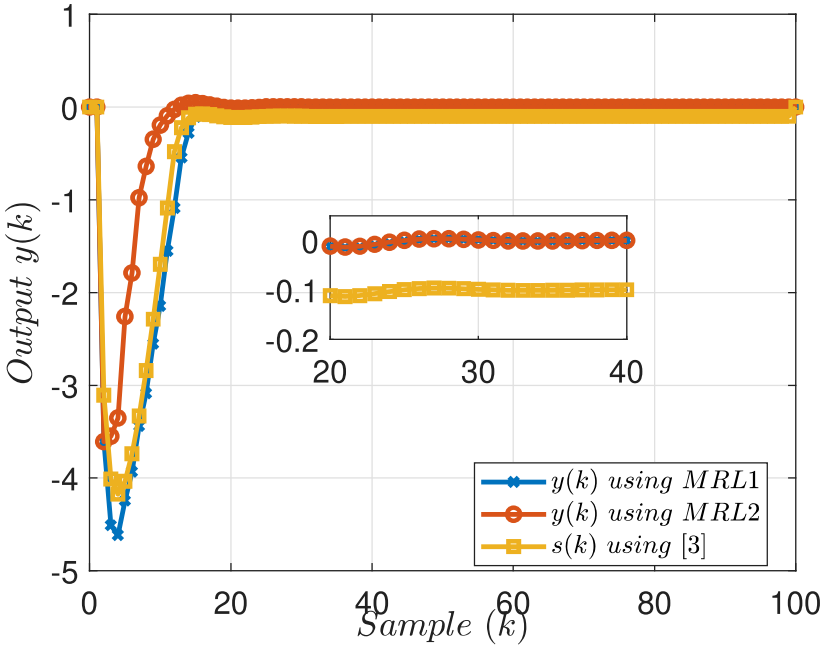

(a) Output comparison

Figure 5.5: Comparative Study of MRL1 , MRL2 and [3]

5.4.3 Experimental Validation

The coupled tank system is used as a test bench. The schematic in Fig. 5.8 illustrates the construction of the system, and Fig. 5.9 shows the actual test bench,

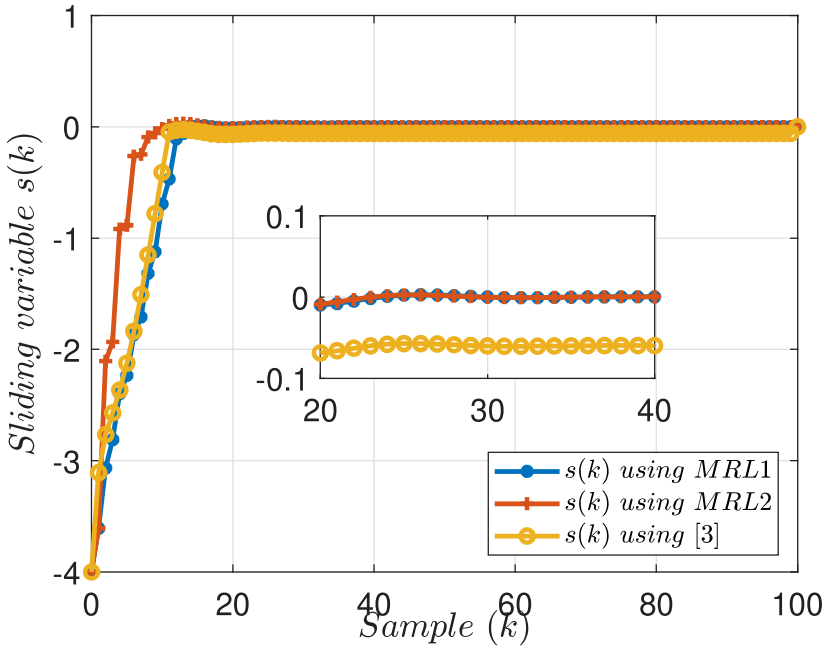

(a) Sliding variable comparison

Figure 5.6: Comparative Study of MRL1 , MRL2 and [3]

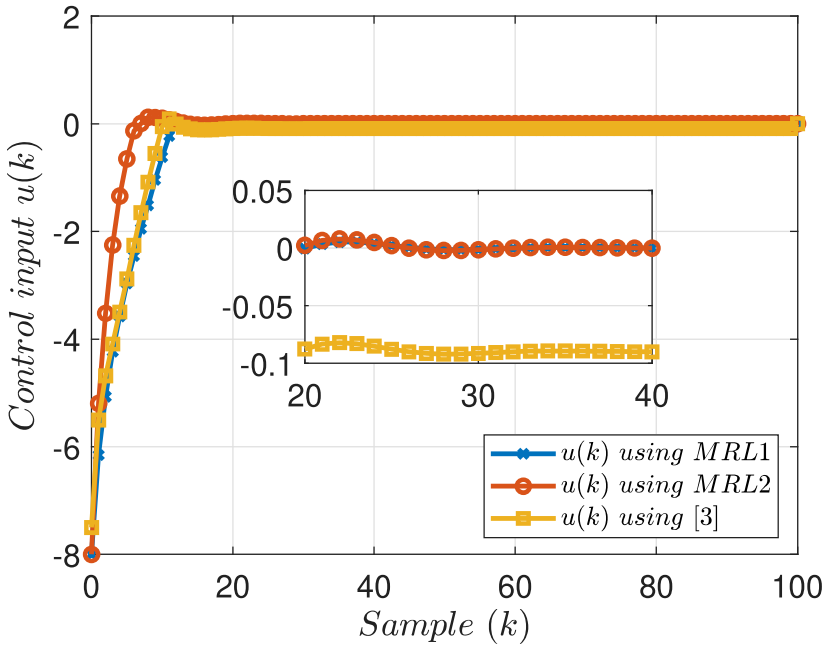

(a) Control input comparison

Figure 5.7: Comparative Study of MRL1 , MRL2 and [3]

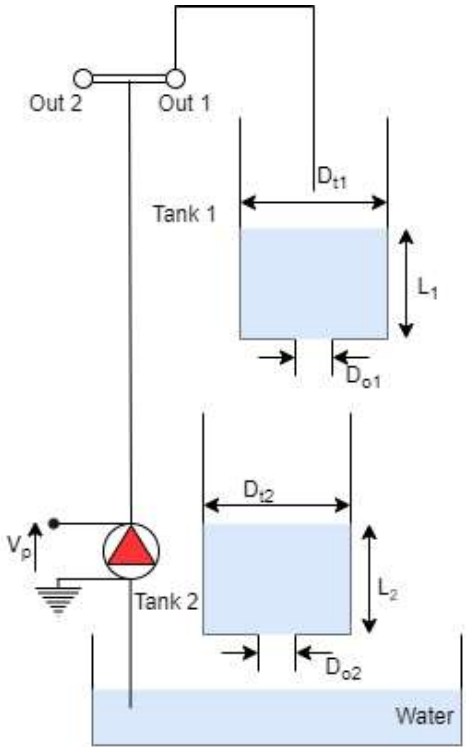

Figure 5.8: Coupled tank block diagram,

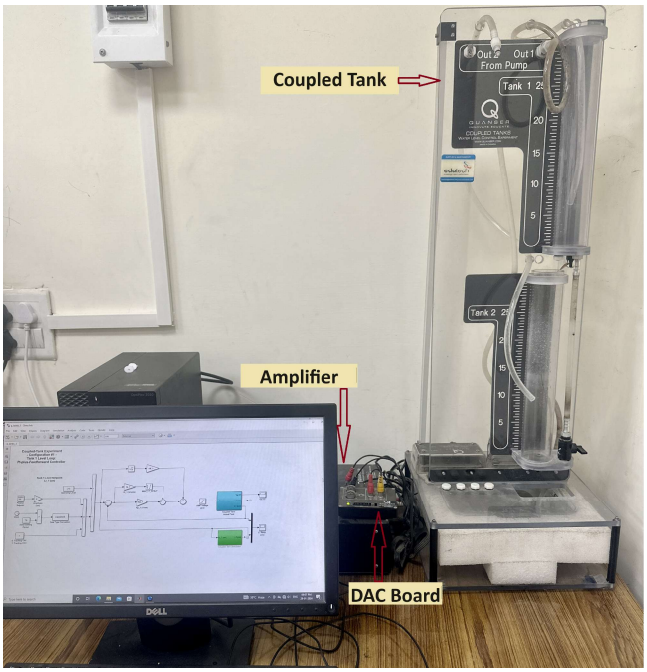

Figure 5.9: Experimental setup coupled tank

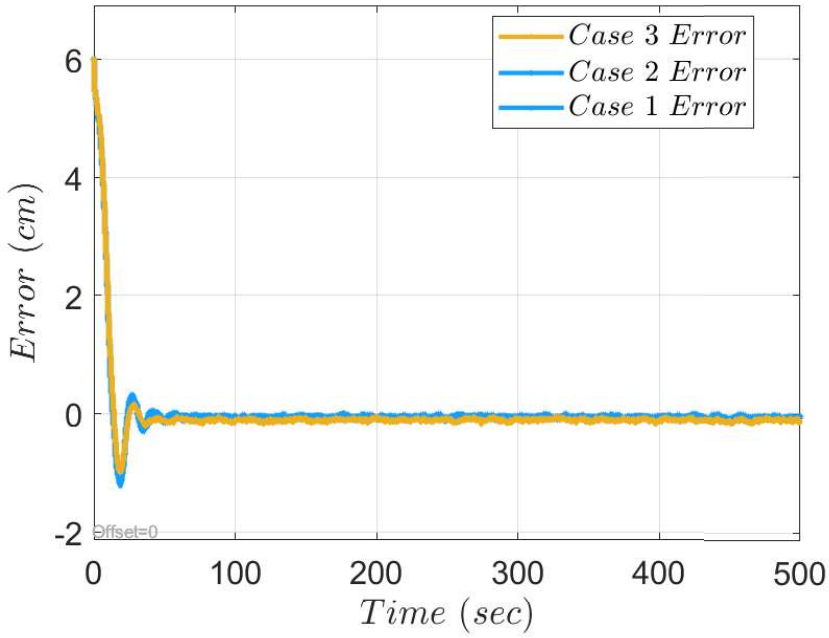

Figure 5.10: Overview of the experimental results of MRL1 scheme for constant hight tracking: Tracking error

Table 5.2: Control parameter for MRL1

Control Parameter	**MRL1**
β	0.1
l_o	0.1
ς	1.1

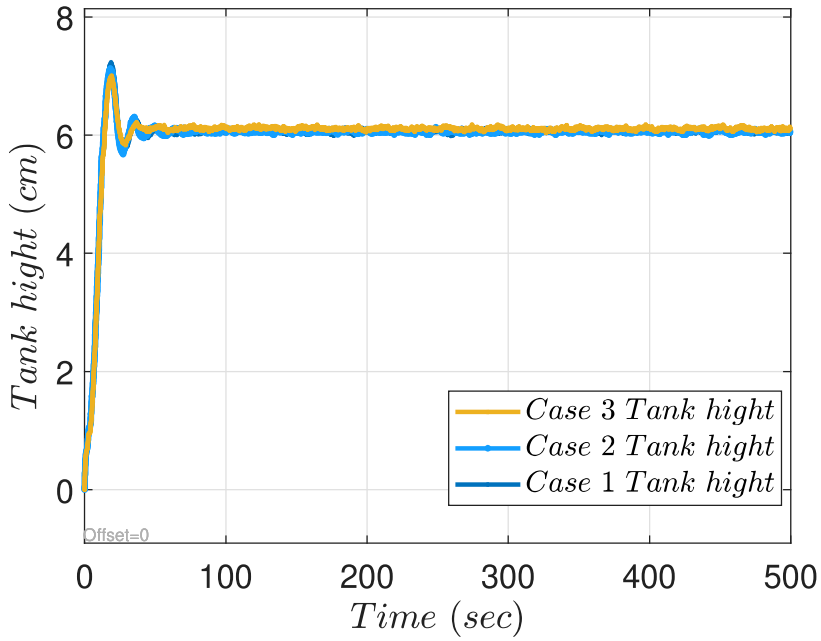

Figure 5.11: Overview of the experimental results of MRL1 scheme for constant hight tracking: Output (tank 2 hight)

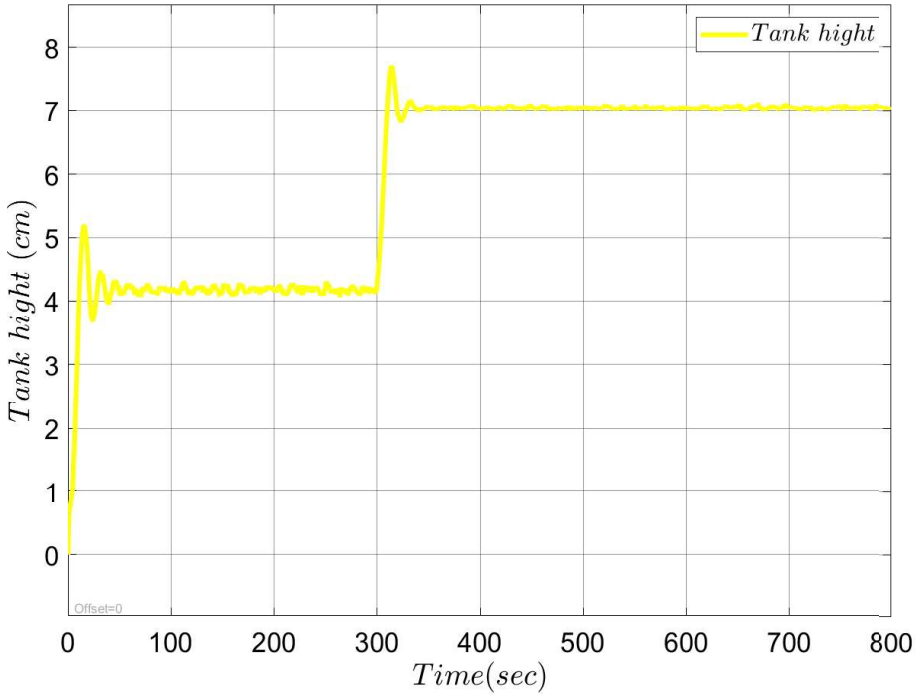

Figure 5.12: Overview of the experimental results of MRL2 scheme for step signal tracking: Tracking error

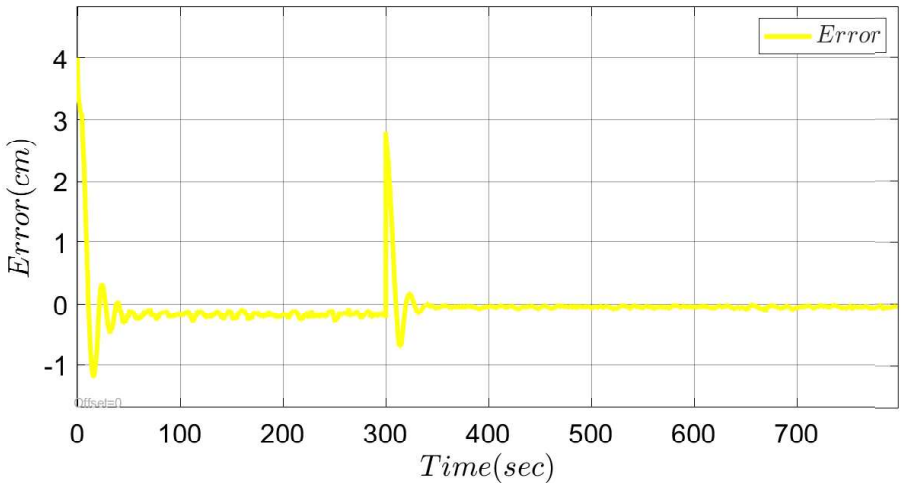

Figure 5.13: Overview of the experimental results of MRL2 scheme for step signal tracking: Output (tank 2 hight)

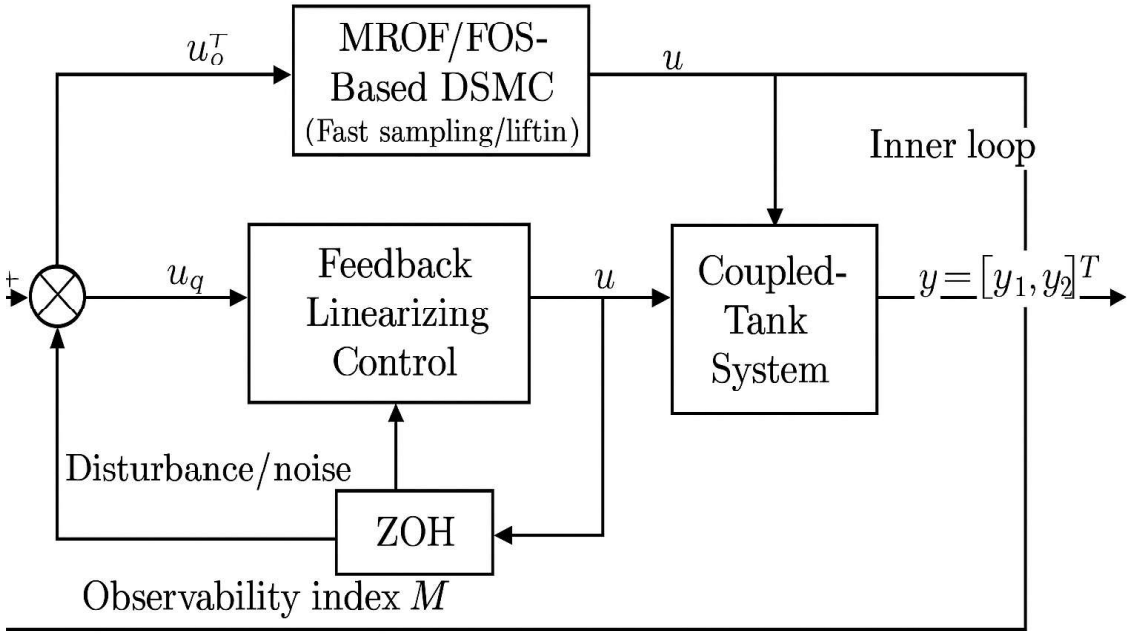

Figure 5.14: Control block diagram for experimental setup

where the control objective is to maintain the desired water level in tank 2 using framework as described in Fig. 5.14. Configuration 2 of the coupled tank system [53] is chosen for the experiments. In this configuration, the control input is applied to the inlet of tank 1, and the outflow of tank 1 acts as a control for tank 2. This setup introduces a coupling effect, where the levels in both tanks are interdependent, adding complexity to the control process. The liquid level is measured by a pressure sensor at the bottom of each tank, providing a linear voltage output that increases with pressure. This signal is processed through a conditioning board and converted to a 0 to $5V$ DC output. The control parameters used for the experimental setup are listed in Table 5.2. For the system parameters reader may refer to [53].

Fig. 5.10 and Fig. 5.11 present the experimental validation of the proposed MRL1 scheme for constant-height tracking, in which the reference levels are achieved within a finite time. In this experiment, the desired height is maintained at 6 cm. Fig. 5.10 illustrates the system error, whereas Fig. 5.11 depicts the desired signal tracking performance for three different cases, each corresponding to a distinct past output sampling conditions:

- Case 1: $\mathbb{M} = 2$,
- Case 2: $\mathbb{M} = 3$,
- Case 3: $\mathbb{M} = 4$.

It is observed that the tracking dynamics vary with the past output sampling conditions, demonstrating the adaptability and robustness of the proposed scheme.

Furthermore, Fig. 5.12 and Fig. 5.13 illustrate the tracking performance for a step reference signal $y_{r,t}$ defined as

$$y_{r,t} = \begin{cases} 4, & t < 300, \\ 7, & t \geq 300. \end{cases}$$

The results confirm that the proposed method ensures smooth and finite-time convergence for both step levels, thereby validating its effectiveness in handling abrupt reference changes.

5.5 Conclusions

A novel control methodology for discrete-time sliding mode control (DSMC) is proposed, integrating a minimum-operator-based reduced-learning sequence (RLs) approach with a multi-rate output feedback (MROF) technique. This hybrid control framework eliminates the need for a switching control input, thereby mitigating the undesirable chattering effects that are typically observed in conventional DSMCs. In contrast to traditional DSMC schemes that depend on full-state feedback, the proposed method utilizes only past output measurements and previous control inputs. This characteristic enhances its suitability for practical applications, where full-state information is often unavailable or challenging to obtain. The incorporation of the multi-rate output feedback mechanism further improves control efficacy and facilitates practical implementation, resulting in enhanced system response characteristics. Comparative analysis with an existing MROF-based output feedback strategy demonstrates that the proposed MRLs approach yields a significant reduction in the quasi-sliding mode band compared with the control algorithm presented in [3], leading to improved precision and robustness. To assess the effectiveness of the proposed scheme, numerical simulations were conducted and benchmarked against the methods reported in [3] and [2]. These simulations evaluate the system behavior under the specified MRLs, showing that the proposed method achieves superior performance in terms of settling time, steady-state error, and robustness against disturbances. Experimental validation was carried out on a coupled-tank system by implementing the developed MRL1 scheme for three different observability indices. The results clearly reveal the influence of the past output sampling conditions on the tracking error. Furthermore, experiments were performed for two distinct scenarios—step reference tracking and constant-height tracking—which further reinforce the proposed method's effectiveness.

Future work will focus on extending the methodology to systems with more pronounced nonlinearities, higher-dimensional dynamics and lightly excited systems.